Brief Communication

Transport of titanium dioxide nanoparticles in saturated porous media under various solution chemistry conditions

Yu Wang[1], Bin Gao[1*], Verónica L. Morales[2], Yuan Tian[1], Lei Wu[1], Jie Gao[3], Wei Bai[3], and Liuyan Yang[5]

1. Department of Agricultural and Biological Engineering, University of Florida, Gainesville, FL 32611-0570, U.S.A.

2. SIMBIOS Centre, University of Abertay, Dundee, DDI U.K.

3. Department of Environmental Engineering Sciences, University of Florida, Gainesville, FL 32611-6450, U. S.A.

4. State Key Laboratory of Pollution Control and Resource Reuse, School of the Environment, Nanjing University, Nanjing 210093, China

---

[*] Corresponding Author, Phone: (352) 392-1864 ext. 285, email: bg55@ufl.edu

Abstract

Because of its wide applications, nanosized titanium dioxide may become a potential environmental risk to soil and groundwater system. It is therefore important to improve current understanding of the environmental fate and transport of titanium oxides nanoparticles (TONPs). In this work, the effect of solution chemistry (i.e., pH, ionic strength, natural organic matter (NOM) concentration) on the deposition and transport of TONPs in saturated porous media was examined in detail. Laboratory columns packed with acid-cleaned quartz sand were used in the experiment as porous media. Transport experiments were conducted with various chemistry combinations, including four ionic strengths, three pH levels, and two NOM concentrations. The results showed that TONP mobility increased with increasing solution pH, but decreased with increasing solution ionic strength. It is also found that the presence of NOM in the system enhanced the mobility of TONPs in the saturated porous media. The Derjaguin-Landau-Verwey-Overbeek (DLVO) theory was used to justify the mobility trends observed in the experimental data. Predictions from the theory agreed excellently with the experimental data.

Keywords: Titanium oxides, nanoparticles, transport, solution chemistry, mobility.

Introduction

In the XXI century alone, large quantities of nanoparticles (NPs) have been introduced into aquatic environments due to the growing production, use and disposal of nano-enabled products. The projections of a rising load of NPs into the environment have raised concerns about their dispersion, as well as their potential toxic effect on specific organisms and on entire ecosystems (Gao et al. 2009; Guzman et al. 2006b; Li et al. 2012; Xiong et al. 2009; Zhang et al. 2009). The small size of NPs makes them highly reactive and toxic to aquatic organisms, as these are small enough to cross cell membranes with ease (Gao et al. 2009; Tervonen et al. 2009). Therefore, suitable understanding of their fate and transport in the environment is required in order to assess the potential risks these particles pose to public and environmental health. From classic filtration theory projections, changes in the size of NP aggregates are expected to affect transport, and solution chemistry conditions are known to affect aggregation. Thus, understanding the link between chemistry-induced aggregation and transport will be critical to assess environmental dispersion of NPs.

Titanium dioxide nanoparticles (TONPs) are among the most widely manufactured/ engineered NPs to date (Kiser et al. 2009). The popularity for TONPs stems from its broad set of applications, including food packaging, cosmetics, sunscreens, paints, and environmental application such as photo-catalyst. The forecasted annual production of TONPs for the year 2025 is 2.5 million tons (Robichaud et al. 2009) with the majority of its application as freely moving nanoparticles (i.e., particles with three dimensions smaller than 100 nm) (Lecoanet et al. 2004).

Only a limited amount of investigations have been conducted to study the environmental fate and transport of TONPs in aqueous systems (Chen et al. 2011; Fang et al. 2009; Guzman et

al. 2006a; Solovitch et al. 2010). These studies have shown that TONP transport and retention in saturated porous media are controlled by multiple factors, including surface properties of the TONPs and the porous medium, solution chemistry (e.g., pH and ionic strength), flow velocity, surfactant concentration, and presence of natural organic matter (NOM) (Chen et al. 2008, 2010; Chowdhury et al. 2011; Domingos et al. 2009; Godinez and Darnault 2011). For example, Solovitch et al. (2010) observed that alkaline conditions promoted greater mobility of TONPs, while increasing ionic strength resulted in great retention in a sandy porous medium. Similarly, Chen et al. (2011) observed that higher ionic strength conditions promoted TONP aggregation and subsequent retention. Alternatively, natural organic matter (NOM) has been shown to increase the stability of TONP suspensions (Fang et al. 2009; Thio et al. 2011).

The overarching objective of this paper was to determine the effect of solution chemistry on the fate and transport of TONPs in saturated porous media. Transport experiments with clean sand packed columns were conducted to test the retention and release of TONPs under various solution chemistry conditions (pH of 7.3, 8.3, and 10.3, ionic strengths of 0.1, 1, 10, and 100 mM, and presence and absence of NOM). The specific objectives were to: 1) determine the stability of TONP suspensions under various solution chemistry conditions, 2) examine the effect of solution chemistry on the retention and transport of TONPs in saturated porous media, 3) examine the effect of transient flow chemistry on TONP release in saturated porous media, and 4) determine the size distribution of TONPs before and after transport experiments.

Materials and Methods

Preparation of TiO2 NPs suspensions and Porous media

Titanium dioxide nanoparticles (Aeroxide TiO_2 P25, Evonik Degussa Corporation, NJ) were used in all experiments. According to the manufacturer, TONPs were more than 99.5% pure with a primary particle size around 30 nm. A stock suspension of TONPs (100mg/L) was prepared by adding the TONP powder into DI water followed by ultrasonication with a Misonix S3000 ultrasonicator (60 minutes). TiO_2 suspensions (10mg/L) were prepared by diluting the stock suspension into prepared solutions of various chemical characteristics of varying pH, ionic strength, and NOM concentration, as indicated in Table 1. This TiO_2 suspension concentration was chosen for the convenience of sample analysis in the transport study. 1 M NaOH and 1 M HNO_3 solutions were used to adjust the solution pH and 1 N $NaNO_3$ solution was used to adjust solution ionic strength. For experiments conducted at pH 7.3 and 8.3, $NaHCO_3$ and Na_2CO_3 were used, respectively, to buffer the suspension pH.   The final TONP suspensions were further sonicated for an additional 10 minutes prior to experimentation. To test the effect of natural organic matter (NOM) on TONP transport, the Suwanee River humic acid (SRHA) (standard II, International Humic Substances Society) was used as a model of NOM. The zeta (ζ) potential of TONPs at each chemical condition was measured by Brookhaven ZetaPlus (Brookhaven Instruments, Holtsville, NY) and the values reported in Table 1.

Quartz sand (Standard Sand & Silica Co.) was used in this study as the porous medium with a size range of 0.5-0.6 mm and approximate average diameter of 0.55 mm. Prior to use, the sand was washed sequentially by tap water, 10% nitric acid (v:v) and nano-pure water. After washing, the sand was then oven-dried at 550 ℃ overnight and stored in a tight container. The purity of the sand was examined using X-ray diffraction (XRD). Details of the XRD are reported

by in a previous study (Tian et al. 2010). The ζ-potential for the sand under different solution chemistry conditions was measured following the method by Johnson et al. (Johnson et al. 1996).

Stability of TPNs in various solution chemistry conditions

Suspension stability and quiescent aggregation was measured for each chemical composition of the TiO$_2$ suspension using a method similar to Fang et al. (2009). Prior to stability measurements, the TiO$_2$ suspensions (10mg/L) were sonicated for 10 minutes to homogenize and monodisperse the samples. To measure stability, 500 mL of a given TiO$_2$ suspension were added to a glass beaker and allowed to settle undisturbed for 4 hours. The duration of quiescent settling was selected to match in time the length of the column experiments. Throughout the settling time, a 5mL aliquot of supernatant liquid was carefully sampled from the top of the beaker (1 cm below surface) every hour, from which the concentration and particle size of TONPs was recorded. The concentration of TONPs was determined by measuring the absorbance of light at a wavelength 286 nm with a UV-visible spectrophotometer (UVS). The calibration curve can be found in the supporting information (Figure S1). The average TONP aggregate size was measured with dynamic light scattering (DLS) (Zetasizer Nano-ZS analyzer, Malven Instrument Inc., U. K) and reported as hydrodynamic diameter. Although only average TONP sizes were reported, size distribution information of TONPs under the tested experimental conditions can be found in the supporting information (Figure S2).

Transport of NPs in porous media

An acrylic column of 2.5 cm in diameter and 16.5 cm in height was wet-packed with clean sand. The porosity of column was approximately 0.41. Once packed, flow in the column

was induced in a downward direction with a peristaltic pump (Masterflex LS, Cole Parmer

Instrument, Vernon Hills, IL). Hydrochemical equilibration was reached by applying 10 pore

volumes (PVs) of DI water followed 10 PVs of background solution through the column at a

constant velocity of 0.5 cm/min. Then, a pulse of stable TONP suspension (10 mg/L) with same

background solution chemistry was injected into column for 2 PVs, followed by 2 PVs TONPs-

free background solution. The effluent of the column was sampled with a fraction collector every

4 minutes and the concentration of the TONP effluent monitored with UVS as described above.

Additionally, a conservative tracer test was conducted with 50 mg/L NaBr solution following the

same conditions for the TONP experiments. The average size of the TONP aggregates in the

effluents was analyzed after 1.8 PV were eluted. Upon completion of the steady-state transport

experiments, three of the columns were subsequently flushed with background solution

conditions different from those used initially (increase in pH, increase in NOM concentration,

and decrease in IS) to create unfavorable conditions for retention and release the deposited

TONPs by a chemical transient. The specific changes in background solution chemistry are listed

in Table 3.

DLVO theory

In this study, a similar method to that used previously by the authors (Tian et al. 2010)

was followed to calculate the DLVO interaction energy. Briefly, the energy profile for sphere-

plate geometry were calculated as the sum of Lifshitz – van der Waals attractive energy (ΔG^{LW})

and electric double layer repulsive energy (ΔG^{EDL}) (Elimelech et al. 1995):

$$\Delta G^{LW} = -\frac{A_{132}}{6}\left[\frac{r}{h} + \frac{r}{h+2r} + \ln(\frac{h}{h+2r})\right] \tag{1}$$

$$\Delta G^{EDL} = 64\pi r \varepsilon \varepsilon_0 \left[\frac{kT}{ze} \right]^2 \tanh \left[\frac{ze\psi_1}{4kT} \right] \tanh \left[\frac{ze\psi_2}{4kT} \right] \exp(-\kappa h) \tag{2}$$

where A_{132} is the Hamaker constant for substances "1" and "2" in presence of medium "3", which can be determined from the Hamaker constant of each material , h is the separation distance, r is the radius of the particle, ε is the dielectric constant of the medium, ε_0 is the vacuum permittivity, k is the Boltzmann's constant, T is the temperature, z is the valence of electrolyte, e is the electron charge, ψ_1 and ψ_2 are the surface potential of the particle and the sand surface, and κ is the reciprocal of the Debye length. The surface potential of TONPs and the sand was calculated from measured ζ-potentials, following the relationship by van Oss et al. (1990):

$$\psi = \zeta (1 + \frac{d}{r}) \exp(\kappa d) \tag{3}$$

where d is the distance between the surface of the charged particle and the slipping plane and usually taken as 5 A (van Oss et al. 1990). The total DLVO interaction energies between the particles and the sand were determined using equations (1) - (3) and normalized with kT.

Results and discussion

Stability of TONP suspensions

The ζ-potential of TONPs and sand at different conditions are presented in Table 1. ζ-potentials of TONPs ranged from -17.76 to -50.45 mV, following trends of increased ζ-potential with ionic strength and decrease with pH, in agreement with previous studies (Thio et al. 2011). The changes to ζ-potential with IS are a result of the expected phenomenon of electrostatic double layer compression by charge screening. Previous studies reported points of zero charge for the sand and TOPNs to be around 3.0 and 6.2, respectively (Suttiponparnit et al. 2011; Tian

et al. 2012). These results indicate that both sand and TONPs have negative charge under the entire range of experimental conditions used in this study.

The stability of TONPs under various conditions was studied in a 4-hour period. The normalized suspension concentration and average particle size of the TONP aggregates at the chemical conditions tested were plotted over time in Figures 1 (a) and (b), respectively. In general, conditions of higher pH and lower IS conditions resulted in more stable TONP suspensions. Two potential mechanisms responsible for the destabilizing effect at higher ionic strength include: 1) reduce surface charge of TONPs and 2) decrease the exponential decay length of electrostatic repulsion (Thio et al. 2011; Zhang et al. 2012). At higher pH, the TONPs have a more negative surface charge, which affords the suspension with electrostatic stability. The normalized TONP concentrations at pH of 7.3 and IS of 1 mM dropped over time for all samples, indicating unavoidable instability for TiO_2 suspensions. However, TONP conditions where NOM was added maintained the steadiest normalized concentration, thus displaying the greatest stability during the measured aging time (Figure 1). After 4 hours, the TONPs sample with pH 8.3 and IS 0.1 mM had the smallest average aggregate size, while the sample at the same pH but IS of 100 mM had the largest average aggregate size (see Figure 1b). All tested solution chemistry conditions allowed the TONPs to remain above 80% the original concentration throughout the 4 hour period, indicating that the stability of the suspensions at the conditions investigated was acceptable.

The aggregate size and ζ-potential measurements of each solution chemistry condition were used to calculate a single collector interaction profiles following classic DLVO theory. For particle-collector interaction profiles, repulsive energy barriers were found for all experimental conditions (Figure 2). The primary maxima height reduced when pH dropped from 8.3 to 7.3 at

constant IS of 1mM. For the tested set of chemical combinations, those at neutral pH have the lowest energy maximum and are therefore the conditions most likely to permit TONPs to overcome the energy barrier and become deposited in the primary minimum (Figure 2). In addition, all conditions with IS greater than or equal to 1 mM were characterized for having secondary energy minima (see Figure 2). For conditions where IS was higher and pH was lowest (pH 7.3 and IS 1mM, see Figure 2), the secondary minimum well was deepest, indicating that at these conditions TONPs could experience reversible deposition by secondary minimum interactions.

Transport of TONPs in saturated porous media

TONP transport experiments were performed by injecting a pulse of TONP suspension at each of the specified background solution chemistries through a saturated sand column. The effluent breakthrough concentrations were monitored throughout each transport experiment and the resulting breakthrough curves (BTCs) presented with normalized concentration and cumulative pore volume in Figure 3a. According to the shapes of the BTCs, it is apparent that conditions of higher ionic strength in the background solution resulted in increased TONPs deposition. This trend is consistent with previous studies of a broad range of colloids and NPs in saturated porous media (Chen et al. 2011; Solovitch et al. 2010; Tian et al. 2012). For the conditions where IS was highest (100mM), the breakthrough was close to zero. The increase in IS increased the ζ-potential of the TONP suspension to -23.51 mV (see Table 1), thus decreasing the magnitude of electrostatic double layer repulsion between TONPs and sand surface by means of reducing the primary maximum height and deepening the secondary minimum well (see Figure 2). These changes to the interaction energy profile illustrate the two types of attractive

10

interaction created where TONPs can become immobilized: primary and secondary energy minimum.

The influence of pH on the TONPs transport was studied in the range from neutral to alkaline pH (7.3, 8.3 and 10.3), as illustrated in Figure 3b. The deposition of TONPs in the column was nearly perfect at pH 7.3 with only 5.6% of the injected colloids recovered in the effluent (see Table 1). In contrast, the deposition of TONPs at pH 10.3 was greatly reduced, with 87% of the injected colloids recovered in the effluent (see Table 2). Although for both conditions, the ζ-potential of both TONPs and the sand was negative, the magnitude of the negative charge of the surfaces in the alkaline conditions was much greater. Base on DLVO interaction energies, conditions at pH 10.3 are more unfavorable for deposition than pH 8.3 and 7.3 due to the greater energy barrier and deeper secondary minimum well. It can be inferred from these interaction profiles that TONPs at pH 7.3 are likely filtered by attachment onto the sand surface due to secondary minimum interactions.

Influence of Humic acid on TONP transport

The presence of NOM significantly decreased the deposition of TONPs (Figure 3c). At pH of 7.3, recovery rate of TONPs increased from 4.3% to 28.5% when 5 mg/L C SRHA was added to the solution (Table 2). These results are consistent with previous findings on enhanced colloid and single-walled carbon nanotube transport in saturated porous columns in the presence of humic substances (Franchi and O'Melia 2003). The ζ-potential of TONPs decreased significantly in the presence of SRHA (from -17.76 to -43.5 mV, see Table 1). Also, the average size in TONPs aggregate increased in the presence of SRHA (from 127 nm to 625 nm, see Table 1). In our results, the average particle size of TONPs increased in the presence of SRHA due to

11

the adsorption of SRHA onto TONP surfaces to form a NOM brush layer that makes the particles 'hairy' and also hydrodynamically larger (Morales et al. 2011; Phenrat et al. 2010). During transport, the average TiO_2 aggregate size increased by 33% after passing through the column in the presence of NOM, as indicated by the change in aggregate size in the influent (625 nm) from that in the effluent (837 nm) in Table 2. Alternatively, the average TiO_2 aggregate size increased by 150% after passing through the column in the absence of NOM, as indicated by the aggregate size in the influent (127 nm) and the effluent (316) in Table 2. The observed changes in aggregate size in the effluent indicate that orthokinetic aggregation is hindered in the presence of NOM, likely due to steric repulsion from the adsorbed NOM macromolecule.

Release of Deposited TONPs

Upon completion of the steady-state transport experiments, three selected columns were flushed with a second TONP-free solution of different chemistry to release retained NPs in a similar fashion as has been done in previous studies (Tian et al. 2010; Tosco et al. 2012). In this study, two chemical conditions of TONP deposition were subjected to chemical transient to induce particle re-entrainment. TONP elution was induced by altering the solution chemistry so as to promote repulsion, via increase in pH, addition of NOM, or decrease in IS, as indicated in Table 3. For the experiment where initial deposition conditions were pH of 8.3 and IS of 100 mM, a reduction in IS to 0.1mM resulted in elution of 3.3 % of the originally injected TONPs. This release of deposited TONPs is likely attributed to elimination of the secondary energy minimum where weak and reversible attraction can be experienced, as has been suggested in previous studies for different colloids and nanoparticles (Solovitch et al. 2010). For the experiment where initial pH was 7.3 and IS was 1mM, an increase in pH to 10.3 resulted in

elution of 4.5 % of the originally injected TONPs. According to the DLVO energy profiles, this remobilization of TONPs was similarly due to a reduction in the secondary energy minimum well depth at higher pH conditions. For experiments where initial pH was 7.3 and IS was 1 mM, addition of NOM resulted in elution of 11.4 % of the originally injected TONPs. The mass recovered from this chemical transient was greater than that observed by changing the pH or IS. However, for this remobilization mechanism, reversible secondary energy minimum deposition cannot fully explain the recovered TONP mass, as the ζ-potential for NOM addition is not as negative as that for the other two transients. Therefore, it is expected that the energy profile for NOM would be more favorable for deposition than the conditions generated by pH of 10.3 or IS of 0.1mM. The authors propose that additional repulsive mechanism maybe involved, such as the formation of NPs-NOM complexes to justify the higher recovery of retained TONPs by addition of NOM.

Effect of TONP size distribution

For the breakthrough samples of each transport experiment, the size distribution of TONP aggregates were analyzed with DLS, as presented in Tables 2 and 3. Overall, the TONP average aggregate sizes in the effluents were much larger than that in the influents. For example, the aggregate size of TONPs in the influent at pH 10.3 was 132 nm, while that in the effluent was 352 nm (see values in Table 2). These results are consistent with classic filtration theory, which predicts smaller particles to have increasingly higher removal efficiencies in saturated porous media when the particle diameter is less than 1000 nm (Yao et al. 1971). A similar trend was also observed in previous studies, where TONPs became much larger after passing through porous media (Chen et al. 2011; Solovitch et al. 2010). It is suggested that smaller particles, particularly

nanosized particles, would have greater diffusion coefficients (Einstein-Stokes equation), which would be the main driving mechanism for mass transfer of TONPs from the liquid phase to the collector surface (Solovitch et al. 2010).

Conclusions

Transports of TONPs in water-saturated porous media were investigated under various solution chemistry conditions. DLVO theory was applied to analyze and interpret the experimental data. The results showed that TONPs have higher mobility with high pH and low IS. Similarly, TONP mobility was readily prompted by the presence of NOM. During the transport, TONP aggregates were formed, and finer particles became favorably retained in the porous medium. In an environmental matrix like a groundwater aquifer, the mobility of TONPs is expected to be greatly controlled by the solution chemistry. Solution IS, pH, as well as NOM concentration should play important roles in their final environmental fate. Perturbation in solution chemistry may not only alter the retention and release patterns of TONPs, but also affect their aggregation and size distributions in soil and groundwater systems.

Acknowledgements

References

Chen GX, Liu XY and Su CM (2011) Transport and Retention of TiO(2) Rutile Nanoparticles in Saturated Porous Media under Low-Ionic-Strength Conditions: Measurements and Mechanisms. Langmuir 27: 5393-5402.

Chen LX, Sabatini DA and Kibbey TCG (2008) Role of the air-water interface in the retention of TiO(2) nanoparticles in porous media during primary drainage. Environ Sci Technol 42: 1916-1921.

Chen LX, Sabatini DA and Kibbey TCG (2010) Retention and release of TiO(2) nanoparticles in unsaturated porous media during dynamic saturation change. J Contam Hydrol 118: 199-207.

Chowdhury I, Hong Y, Honda RJ and Walker SL (2011) Mechanisms of TiO(2) nanoparticle transport in porous media: Role of solution chemistry, nanoparticle concentration, and flowrate. J Colloid Interf Sci 360: 548-555.

Domingos RF, Tufenkji N and Wilkinson KJ (2009) Aggregation of Titanium Dioxide Nanoparticles: Role of a Fulvic Acid. Environ Sci Technol 43: 1282-1286.

Elimelech M, Gregory J, Jia X and Williams RA: 1995, 'Particle deposition and aggregtion: measurement, modeling and simulation', Butterworth-Heinemann Ltd.

Fang J, Shan XQ, Wen B, Lin JM and Owens G (2009) Stability of titania nanoparticles in soil suspensions and transport in saturated homogeneous soil columns. Environ Pollut 157: 1101-1109.

Franchi A and O'Melia CR (2003) Effects of natural organic matter and solution chemistry on the deposition and reentrainment of colloids in porous media. Environ Sci Technol 37: 1122-1129.

Gao J, Youn S, Hovsepyan A, Llaneza VL, Wang Y, Bitton G and Bonzongo JCJ (2009) Dispersion and Toxicity of Selected Manufactured Nanomaterials in Natural River Water Samples: Effects of Water Chemical Composition. Environ Sci Technol 43: 3322-3328.

Godinez IG and Darnault CJG (2011) Aggregation and transport of nano-TiO(2) in saturated porous media: Effects of pH, surfactants and flow velocity. Water Res 45: 839-851.

Guzman KAD, Finnegan MP and Banfield JF (2006a) Influence of surface potential on aggregation and transport of titania nanoparticles. Environ Sci Technol 40: 7688-7693.

Guzman KAD, Taylor MR and Banfield JF (2006b) Environmental risks of nanotechnology: National nanotechnology initiative funding, 2000-2004. Environ Sci Technol 40: 1401-1407.

Johnson PR, Sun N and Elimelech M (1996) Colloid transport in geochemically heterogeneous porous media: Modeling and measurements. Environ Sci Technol 30: 3284-3293.

Kiser MA, Westerhoff P, Benn T, Wang Y, Perez-Rivera J and Hristovski K (2009) Titanium Nanomaterial Removal and Release from Wastewater Treatment Plants. Environ Sci Technol 43: 6757-6763.

Lecoanet HF, Bottero JY and Wiesner MR (2004) Laboratory assessment of the mobility of nanomaterials in porous media. Environ Sci Technol 38: 5164-5169.

Li X, Lenhart JJ and Walker WW (2012) Aggregation Kinetics and Dissolution of Coated Silver Nanoparticles. Langmuir 28: 1095-1101.

Morales VL, Sang WJ, Fuka DR, Lion LW, Gao B and Steenhuis TS (2011) Correlation Equation for Predicting Attachment Efficiency (alpha) of Organic Matter-Colloid Complexes in Unsaturated Porous Media. Environ Sci Technol 45: 10096-10101.

Phenrat T, Song JE, Cisneros CM, Schoenfelder DP, Tilton RD and Lowry GV (2010) Estimating Attachment of Nano- and Submicrometer-particles Coated with Organic Macromolecules in Porous Media: Development of an Empirical Model. Environ Sci Technol 44: 4531-4538.

Robichaud CO, Uyar AE, Darby MR, Zucker LG and Wiesner MR (2009) Estimates of Upper Bounds and Trends in Nano-TiO(2) Production As a Basis for Exposure Assessment. Environ Sci Technol 43: 4227-4233.

Solovitch N, Labille J, Rose J, Chaurand P, Borschneck D, Wiesner MR and Bottero JY (2010) Concurrent Aggregation and Deposition of TiO(2) Nanoparticles in a Sandy Porous Media. Environ Sci Technol 44: 4897-4902.

Suttiponparnit K, Jiang JK, Sahu M, Suvachittanont S, Charinpanitkul T and Biswas P (2011) Role of Surface Area, Primary Particle Size, and Crystal Phase on Titanium Dioxide Nanoparticle Dispersion Properties. Nanoscale Research Letters 6:

Tervonen T, Linkov I, Figueira JR, Steevens J, Chappell M and Merad M (2009) Risk-based classification system of nanomaterials. J Nanopart Res 11: 757-766.

Thio BJR, Zhou DX and Keller AA (2011) Influence of natural organic matter on the aggregation and deposition of titanium dioxide nanoparticles. J Hazard Mater 189: 556-563.

Tian Y, Gao B, Wang Y, Morales VL, Carpena RM, Huang QG and Yang LY (2012) Deposition and transport of functionalized carbon nanotubes in water-saturated sand columns. J Hazard Mater 213: 265-272.

Tian YA, Gao B, Silvera-Batista C and Ziegler KJ (2010) Transport of engineered nanoparticles in saturated porous media. J Nanopart Res 12: 2371-2380.

Tosco T, Bosch J, Meckenstock R and Sethi R (2012) Transport of ferrihydrite nanoparticles in saturated porous media: role of ionic strength and flow rate. Environ Sci Technol DOI: 10.1021/es202643c:

van Oss CJ, Giese RF and Costanzo PM (1990) DLVO and Non-DLVO Interactions in Hectorite. Clay Clay Miner 38: 151-159.

Xiong Z, He F, Zhao DY and Barnett MO (2009) Immobilization of mercury in sediment using stabilized iron sulfide nanoparticles. Water Res 43: 5171-5179.

Yao KM, Habibian MM and Omelia CR (1971) Water and Waste Water Filtration - Concepts and Applications. Environ Sci Technol 5: 1105-&.

Zhang HY, Smith JA and Oyanedel-Craver V (2012) The effect of natural water conditions on the anti-bacterial performance and stability of silver nanoparticles capped with different polymers. Water Res 46: 691-699.

Zhang Y, Chen YS, Westerhoff P and Crittenden J (2009) Impact of natural organic matter and divalent cations on the stability of aqueous nanoparticles. Water Res 43: 4249-4257.

Tables

Table 1. Summary of experimental conditions.

Experiment No.	IS (mM/L)	pH	NOM conc. (mg/L)	Zeta potential of TONPs (mV)	Zeta potential of sand (mV)
1	0.1	8.3	0	-40.21	-25.20
2	1	8.3	0	-32.21	-23.45
3	10	8.3	0	-31.97	-20.10
4	100	8.3	0	-23.51	-18.40
5	1	7.3	0	-17.76	-20.19
6	1	10.3	0	-50.45	-29.42
7	1	7.3	5	-43.50	-23.56

Table 2. Summary of experimental results of TONP transport through the columns.

Experiment No.	Influent particle size (nm)	effluent particle size (nm)	Recovery rate (%)
1	90	367	75.9
2	118	347	53.0
3	158	359	27.0
4	169	n/a	1.0
5	127	316	4.3
6	132	352	84.2
7	625	837	28.5

Table 3. Summary of experimental conditions and results of TONP release in the columns.

Experiment No.	Chemistry of the flushing solution			Recovery rate (%)	Released particle size (nm)
	IS (mM/L)	pH	NOM conc. (mg/L)		
4	0.1	8.3	0	3.0	214
5	1	10.3	0	4.5	302
5	1	7.3	5	11.4	713

Figure Captions

Figure 1. Effect of solution chemistry on stability of TONP suspensions: (a) normalized TONP

concentration and (b) average particle size.

Figure 2. DLVO energy profiles between TONPs and sand under various solution chemistry

conditions: (a) pH and (b) IS.

Figure 3. Effect of solution IS (a), pH (b), and NOM concentration (c) on retention and transport

of TONPs in the columns.

Figure 4. Effect of perturbation in solution chemistry on TONP release in the columns.
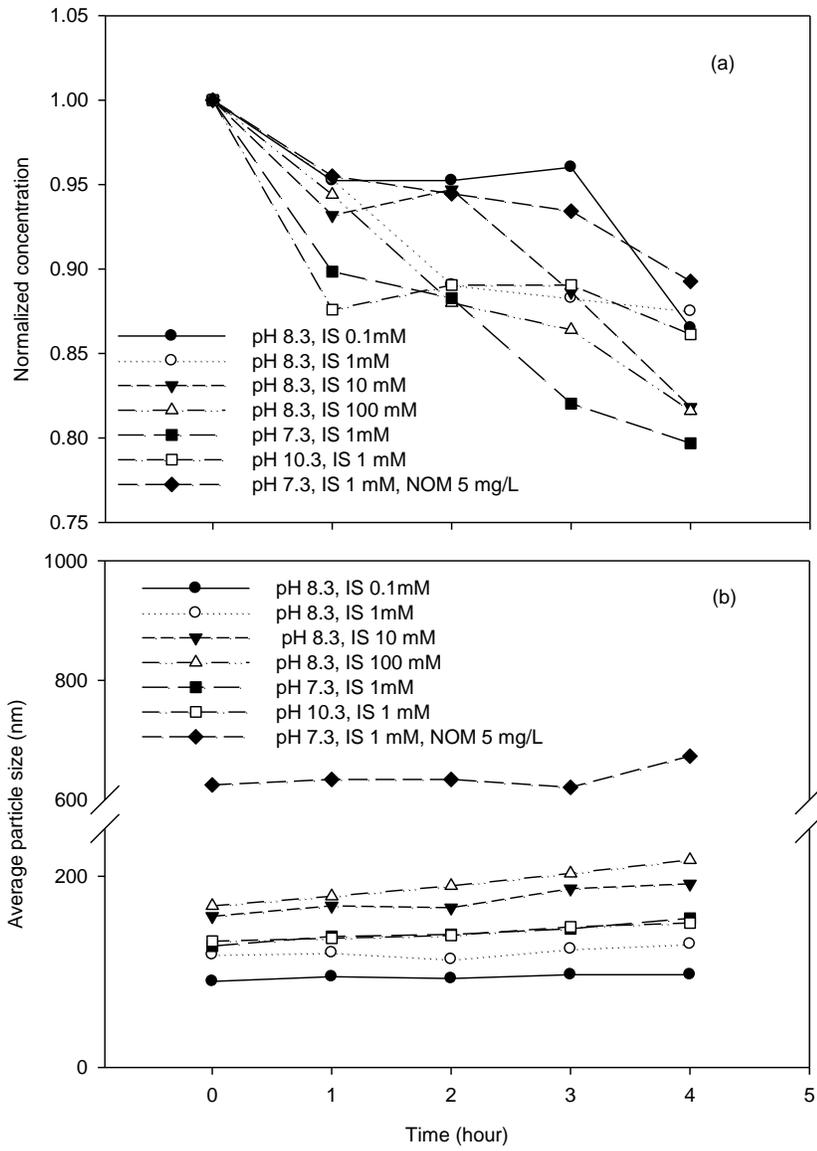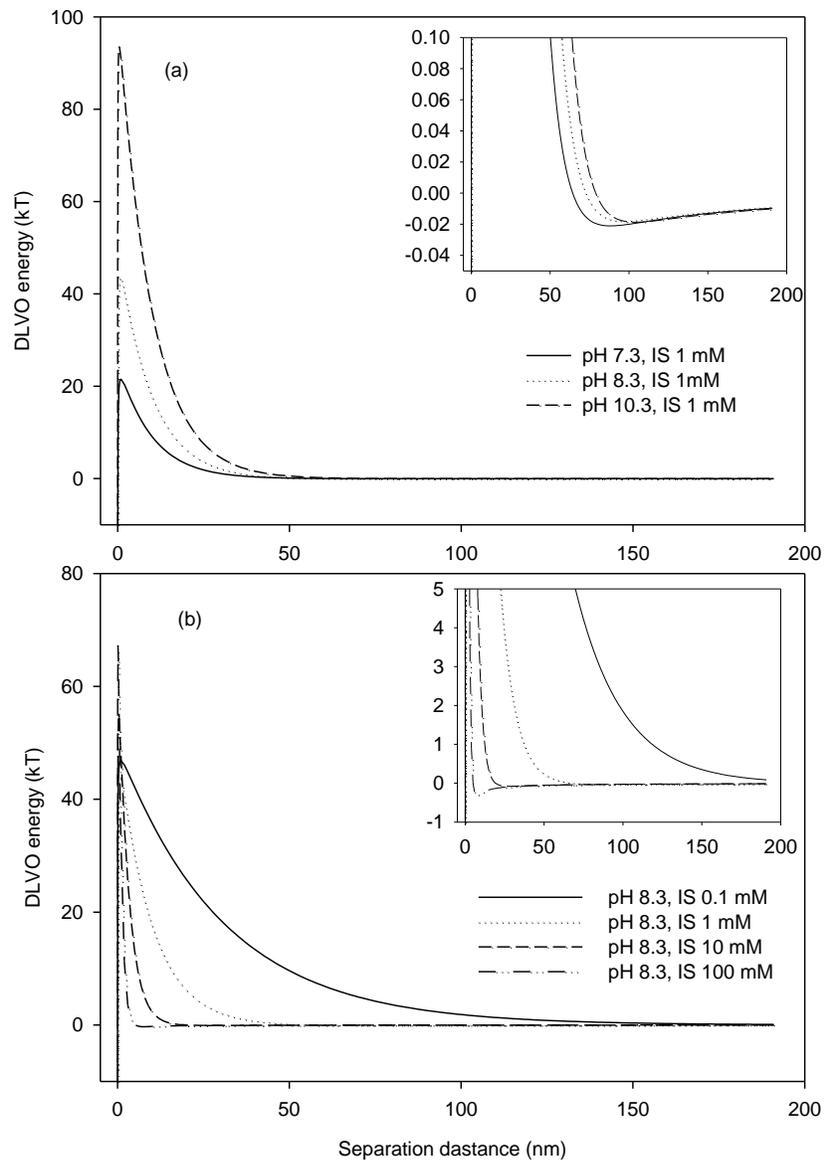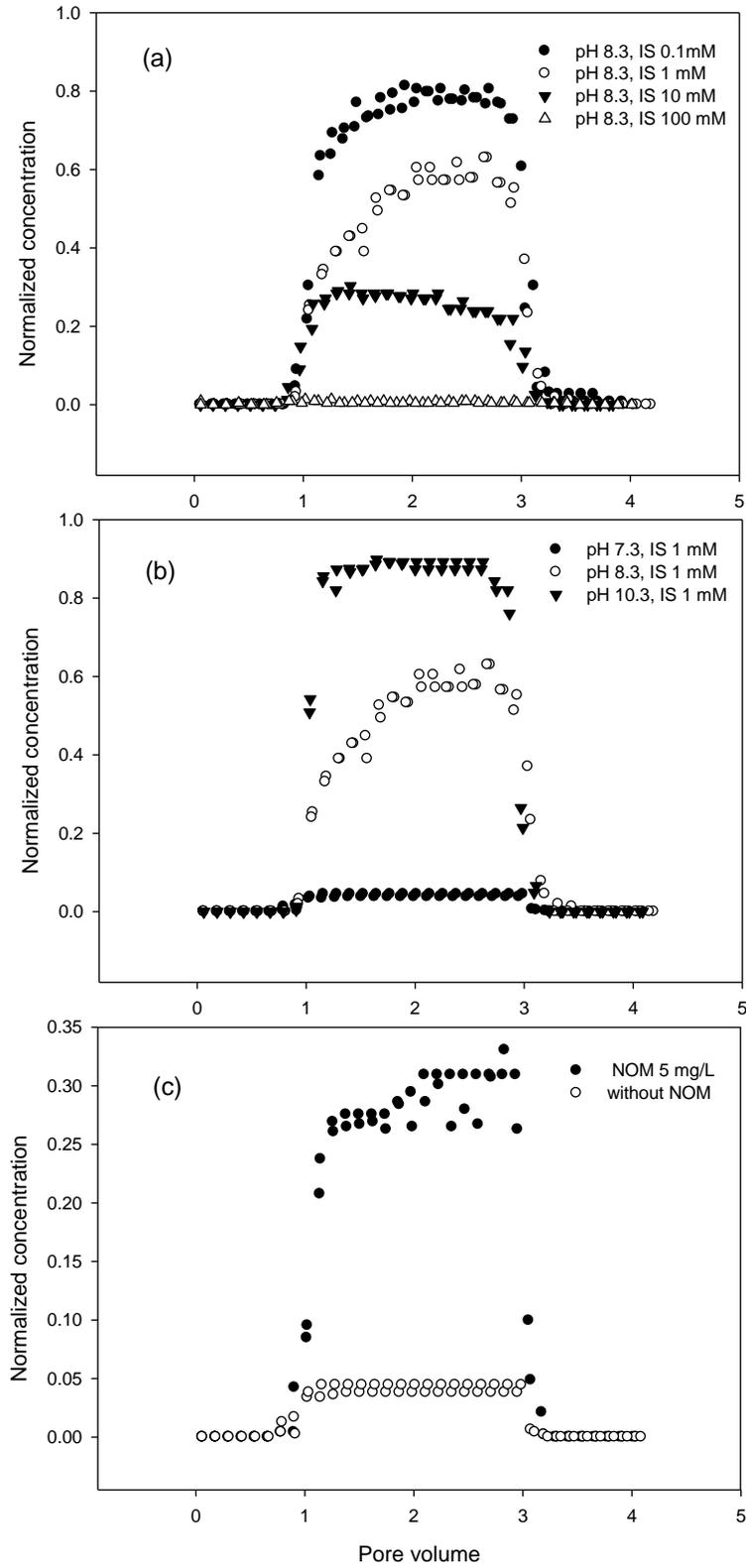
Figure 1.

Figure 2.

Figure 3.

Figure 4.